ADVANCED MATERIALS

Supporting Information

for *Adv. Mater.*, DOI: 10.1002/adma.201903513

Validating a Predictive Structure–Property Relationship by Discovery of Novel Polymers which Reduce Bacterial Biofilm Formation

*Adam A. Dundas, Olutoba Sanni, Jean-Frédéric Dubern, Georgios Dimitrakis, Andrew L. Hook, Derek J. Irvine, Paul Williams, and Morgan R. Alexander**

Supporting Information

Validating a Predictive Structure–Property Relationship by Discovery of Novel Polymers which Reduce Bacterial Biofilm Formation

Adam A. Dundas, Olutoba Sanni, Jean-Frédéric Dubern, Georgios Dimitrakis, Andrew L. Hook, Derek J. Irvine**, Paul Williams** and Morgan R. Alexander**

Supplementary Experimental Methods

Characterisation *via* Nuclear Magnetic Resonance Spectroscopy: ^{1}H and ^{13}C NMR spectroscopic analyses were recored at 25 °C using Bruker AV-400 MHz spectrometers. Samples were dissolved in deuterated chloroform ($CDCl_3$; 10 mg ml^{-1}) to which chemical shifts are referenced (residual chloform at 7.26 ppm). Analysis of the spectra was carried out using MestReNova.

Polymer Microarray Formation: Slides were prepared by dip-coating epoxy-coated glass slides (Genetix) into a 4 % (w/v) poly(hydroxyethyl methacrylate) solution in ethanol. Slides were left to dry in ambient conditions for 24 h and then under vacuum for a week. Polymer microarrays were formed using a XYZ3200 dispensing workstation (Biodot) at 25 ˚C, 30-40 % humidity and less than 0.2 % O_2 levels. Quilled metal pins (946MP6B, Arrayit) were used to transfer monomer solutions (with 1 % (w/v) photoinitiator (2,2 dimethoxy-2-phenylacetonphenone)) onto 10 pHEMA-coated slides and irradiated with UV light.[1, 2] Microarray slides were allowed to dry for a week under vacuum before bacterial screening. Due to having drastically different structure from materials used for the *alpha* model, [2-(Methacryloyloxy)ethyl]dimethyl-(3-sulfopropyl) ammonium hydroxide (MedMPNH) (a

zwitterionic material) could not be reliably predicted using the model but was included on the array for comparison purposes.

Bacterial Biofilm Formation: Bacterial biofilm formation assays were conducted as previously described.[4] Briefly, UV-sterilized polymer coupons or polymer-coated catheters segments were incubated with bacteria at 37˚C with 60 rpm shaking for 72 h in Artificial Urine (AU) [3].The composition of AU was*:* Peptone L37 (1 g/l), yeast extract (0.005 g/l); lactic acid (0.1 g/l); citric acid (0.4 g/l); sodium bicarbonate (2.1 g/l); urea (10 g/l); uric acid (0.07 g/l); creatinine (0.8 g/l); calcium chloride.$2H_2O$ (0.37 g/l); sodium chloride (5.2 g/l); iron II sulfate.$7H_2O$ (0.0012 g/l); magnesium sulfate. $7H_2O$ (0.49 g/l); sodium sulfate.$10H_2O$ (3.2 g/l); potassium dihydrogen phosphate (0.95 g/l); di-potassium hydrogen phosphate (1.2 g/l); ammonium chloride (1.3 g/l). Peptone and yeast extract were obtained from Oxoid, Basingstoke and all other reagents were obtained from SIGMA-ALDRICH, Welwyn Garden city, UK. The pH of AU was adjusted to 6.5.

Air-dried samples were examined using a Carl Zeiss LSM 700 laser scanning confocal microscope fitted with 405 nm, 488 nm and 555 nm excitation lasers and a 10x/NA 0.3 objective. Silver hydrogel catheter sections were cut from Bardex® I.C. Aquafil with a hydrogel and silver alloy coated catheters and silicone catheter sections cut from silicone catheters (Bard Medical, U.K.). Images were acquired using ZEN 2009 imaging software (Carl Zeiss). Bacterial surface coverage was quantified using Image J 1.44 software (National Institutes of Health, USA) and Comstat B. For single-species biofilm formation, polymer coated catheters sections were incubated with AU (20 ml) containing 1 µM (Syto64) and/or 2µM calcein (Sigma) and inoculated with *Pr. mirabilis, P. aeruginosa, S. aureus, E. faecalis, K. pneumoniae* or *UPEC* cells at an OD_{600} of 0.01. Biomass was quantified using confocal

fluorescence microscopy. For mixed-species biofilms, polymer coated coverslips were incubated with AU (20ml) and inoculated with *P. aeruginosa* and *S. aureus* mixed in a 1:10 ratio.

Bacterial Biofilm Formation on Microarrays: Bacterial biofilm formation assays were conducted as previously described.[4] Microarray slides were UV sterilized for 10 min and inoculated (OD_{600} = 0.01) with either m-cherry tagged *P. aeruginosa or* ds-red tagged *Pr. mirabilis* in 20 mL of RPMI-1640 medium contained in a petri dish incubated for 24 h at 37 ˚C at 60 rpm shaking. Control slides were also incubated in the same conditions without bacteria. After incubation, slides were twice rinsed with phosphate-buffered saline at room temperature for 5 min and then with distilled water for 5 min. Fluorescence images were then taken of both control slides and bacteria-exposed slides using a GenePix Autoloader 4200AL (Molecular Devices, US) scanner with a 655 - 695 nm filter. Fluorescence signals from the polymer spots were acquired for each bacterial pathogen by subtracting the fluorescence of the control slide from the fluorescence of the slide exposed to bacteria, which directly correlates with attachment and biofilm formation on the polymer surface. Fluorescence data was acquired using two polymer microarrays with n = 3 triplicates on each (one with bacteria and one microarray as a background control).

CyDMA Polymerisation: 500 mg of purified CyDMA monomer was added to a 5 ml reaction vessel with 500 μL of toluene. 5 mg of azobisisobutyronitrile (AIBN) thermal initiator was then added as a radical initiator for the reaction, which was performed at 80 ˚C for 4 h. This led to a 60% conversion of the monomer to polymer. The crude reaction mixture was

precipitated into methanol twice to remove any un-reacted monomer and remaining solvent and dried in a vacuum oven prior to analysis and application testing.

Supporting Figures

Four non-commercially available monomers with cyclic, aromatic, linear and branched moieties were synthesized using a transesterification method. These monomers were selected to test the *alpha* parameter by providing a range of different hydrocarbon structures and also included a range of predicted values outside reported ranges (CyDMA, LMMA). A nitrogen sparge was utilized to displace the butanol byproduct and help overcome the mass-transfer effect, which in turn allowed for conversions greater than 80 % for three monomers included into monomer library for high throughput screening with polymer microarrays (**Error! Reference source not found.c**). LMMA had a lower conversion of 69 % after 50 hours when compared to CyDMA, GeMA and DdMA all of which were above 80 % just after 3 hours. One of possible reasons for this lower yield is the steric hindrance conferred by isopropyl and methyl substituents on the cyclohexyl ring. Secondly, these substituents also contribute to electron stability of ring.

a

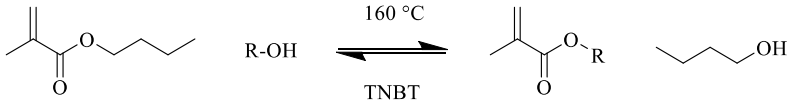

b

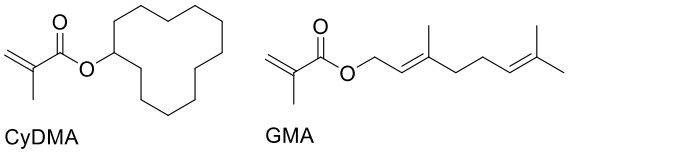

CyDMA GMA

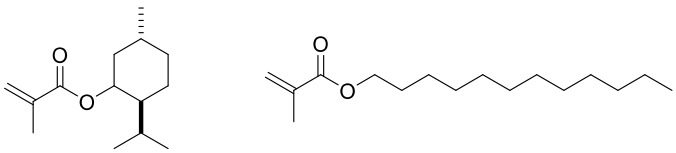

LMMA DdMA

c

Material	Conversion (%)	Prediction
CyDMA	92	-5.47
GeMA	84	-2.13
LMMA	69	-3.51
DDMA	92	-1.47

Figure S1: (a) Reaction sequence used for synthesising novel methacrylate monomers at reaction temperatures of 160 ˚C using a nitrogen gas sparge to enhance reaction kinetics. (b) structures of synthesised materials showing a range of hydrocarbon structures (c) conversion levels of synthesised materials with associated *alpha* prediction values

NMR was used to analyse experiments and to confirm the purity of samples. Analysis was done by observing the chemical shift of protons next to the ester functionality of the product monomer and resulting NMRs can be shown below.

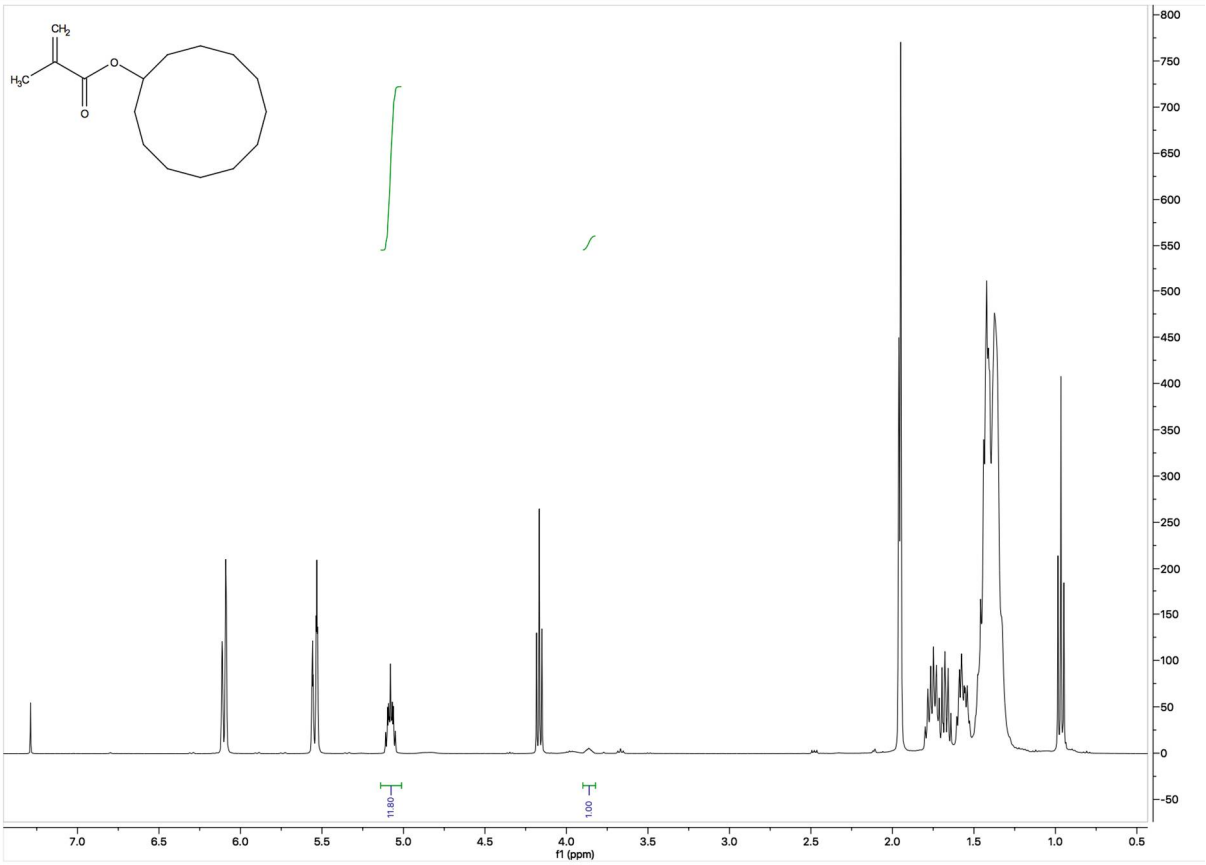

Figure S2: 1H NMR of CyDMA used for polymer microarray experiments, where change in chemical environment from proton in cyclododecanol was used to calculate conversion of monomer. Final conversion was calculated to be 92 %.

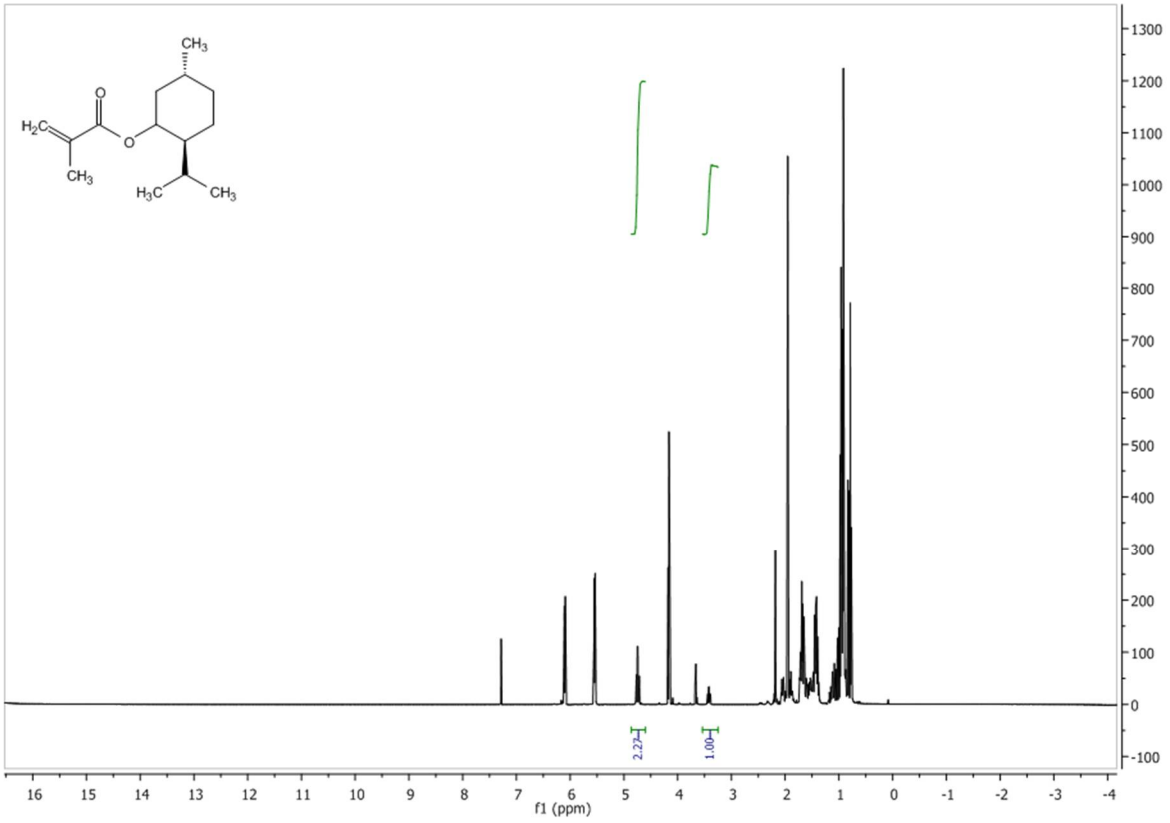

Figure S3: 1H NMR of LMMA used for polymer microarray experiments, where change in chemical environment from proton in l-menthol was used to calculate conversion of monomer. Calculated conversion was found to be 69 %

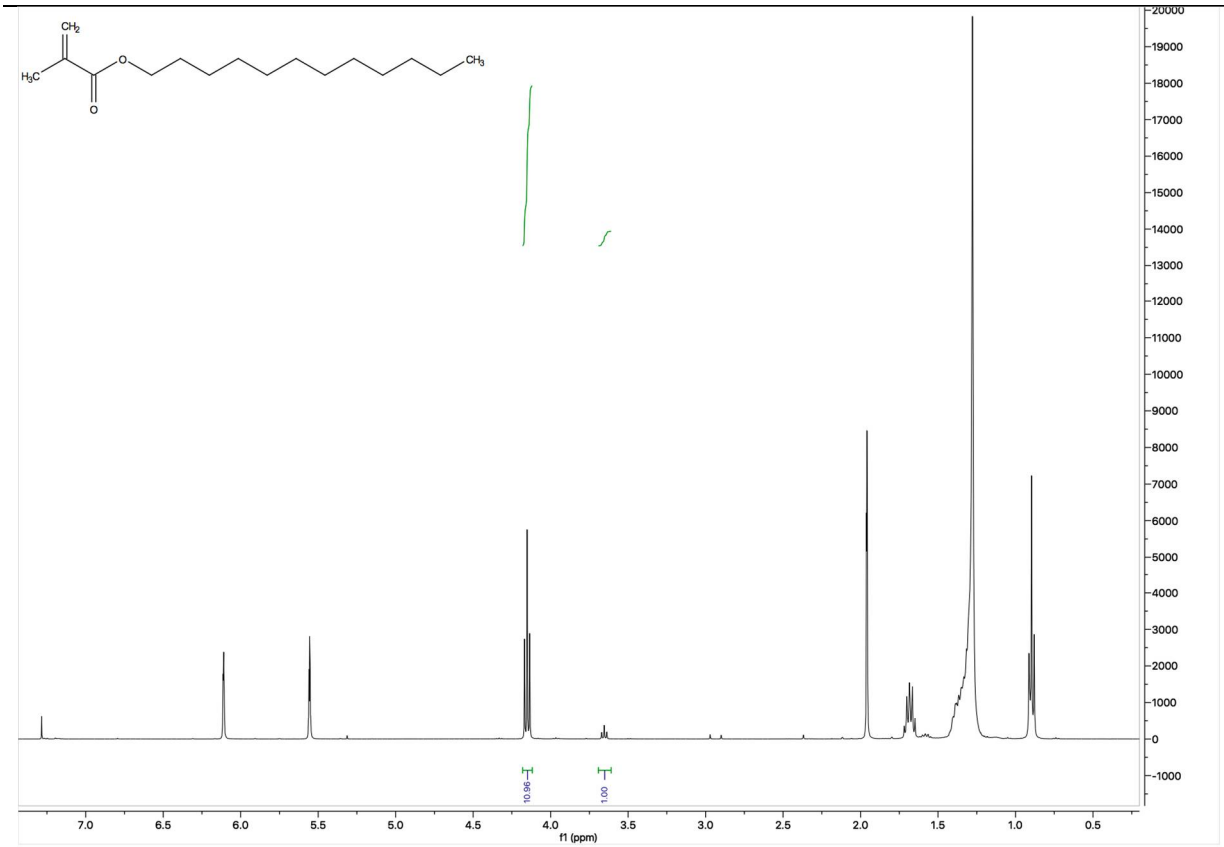

Figure S4: 1H NMR of DdMA used for polymer microarray experiments, where change in chemical environment from proton in dodecanol was used to calculate conversion of monomer. Calculated conversion was found to be 92 %

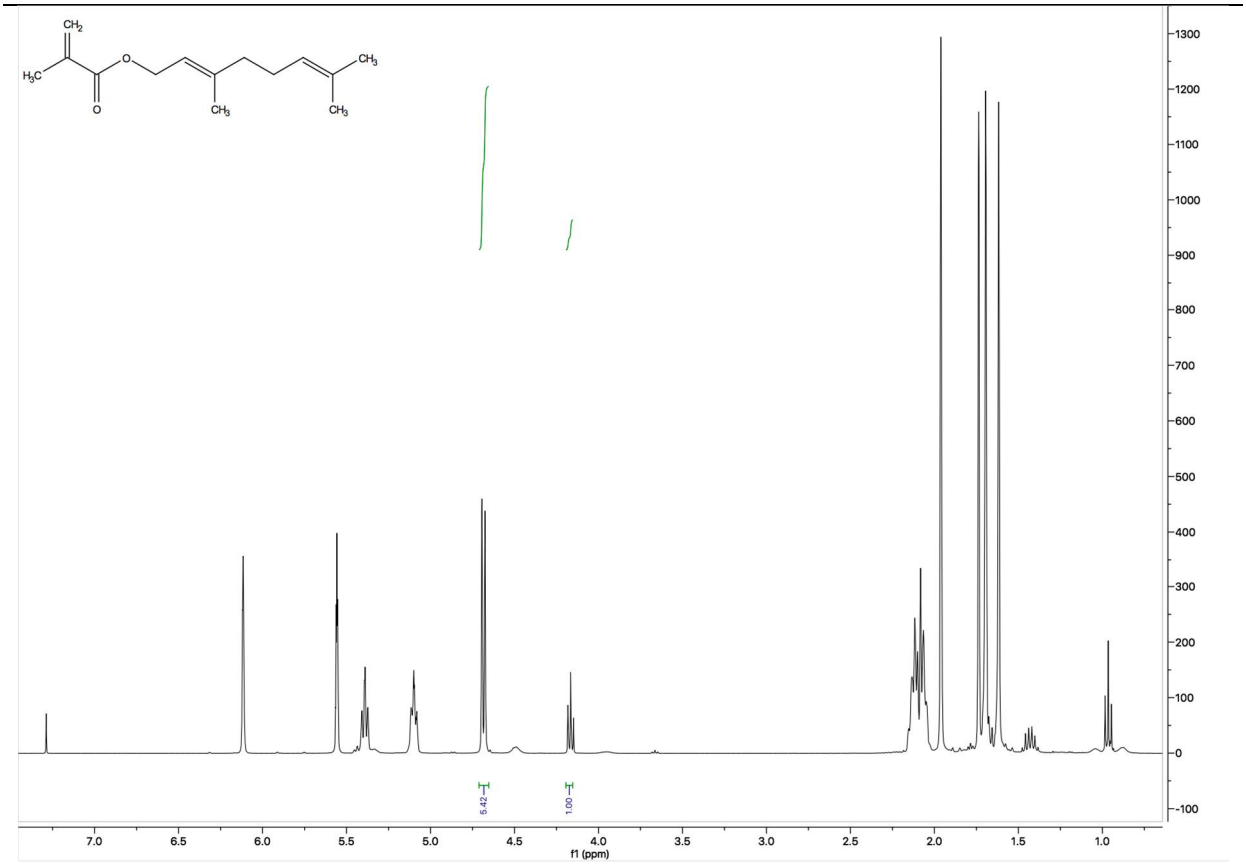

Figure S5: 1H NMR of GeMA used for polymer microarray experiments, where conversion calculated by comparing CH_3 peak from BMA to CH_2 peak next to ester group in GeMA. Calculated conversion was found to be 84 %

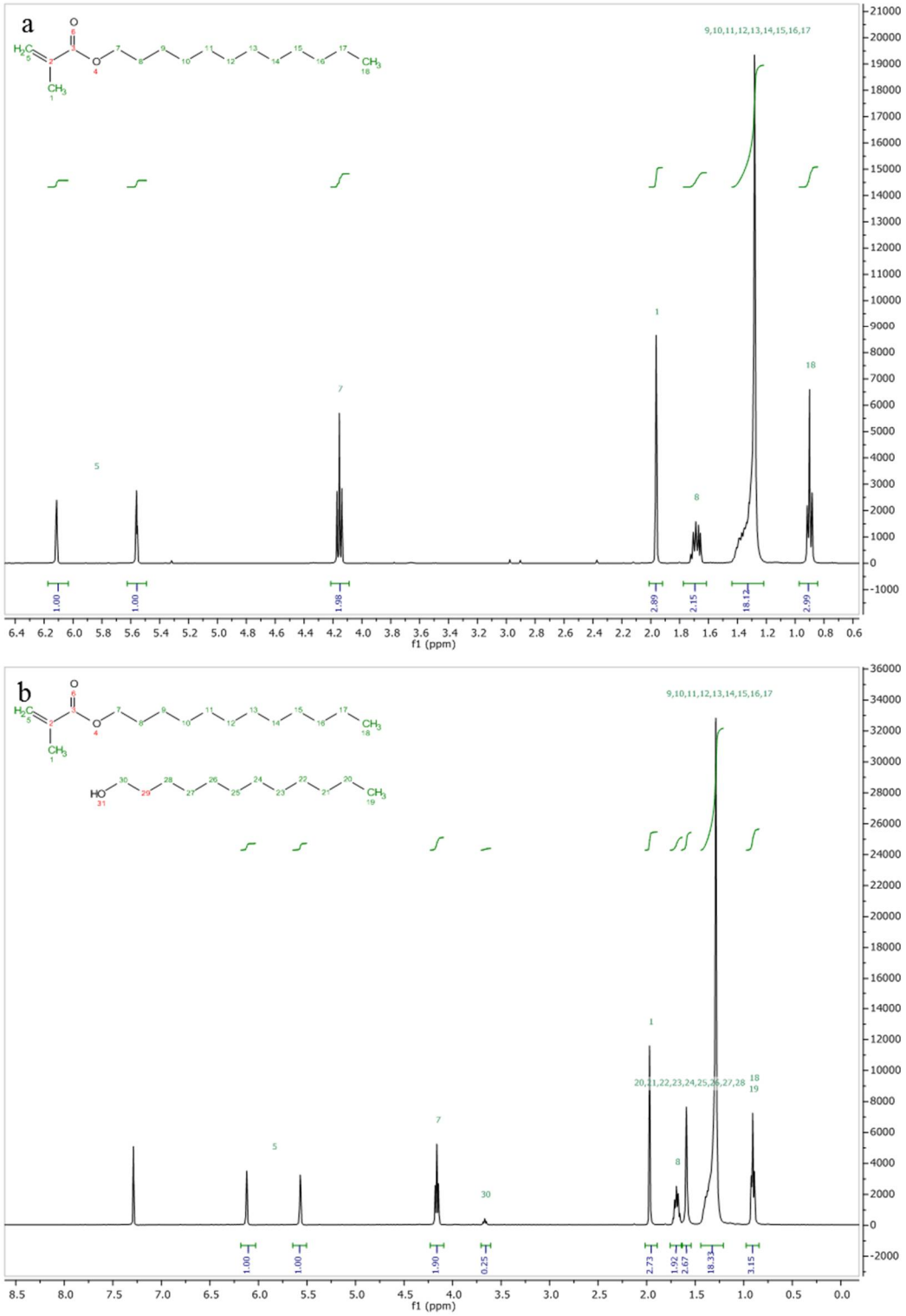

Figure S6: 1H NMR showing differences between (a) commercial DdMA with unknown contaminant showing peaks between 2.2 and 3.2 ppm and (b) synthesised DdMA with known dodecanol contaminant

ToF-SIMS analysis of the polymer microarray also showed key differences in the spectra of the commercial and synthesised DdMA samples. By calculating the differences of the spectra, the contaminant C3H5NO2- was shown to be more prevalent in the commercially available material, showing further evidence of contamination. To observe this effect on a larger scale, samples of both commercially available and synthesised DdMA were deposited onto a methacrylate silanised glass surface and UV photopolymerised in the same method as for polymer microarray printing. This showed a high deviation of bacterial adhesion properties between different samples of commercial DdMA, further suggesting that contamination within the sample could be causing a change in bacterial performance.

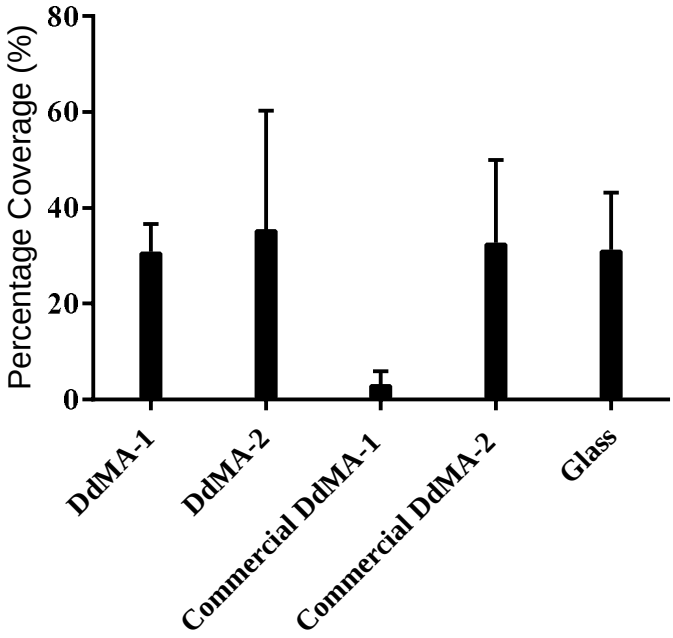

Figure S7: Bacterial performance of scaled-up commercial and synthesised DdMA on methacrylate silanised glass surface, showing large deviation of bacterial performance with commercial sample

In order to observe trends for a copolymer series between *alpha* and bacterial adhesion, ToF-SIMS was used to analyse the surface chemistry of the polymer microarray spots. This was

used to see if the materials within a copolymer series had mixed correctly and hence can be expected to follow the trend set out by *alpha*. Polymers that had a mixing ratio correlation of less than $R^2 = 0.8$ were excluded As shown in **Figure S8**, copolymer series including EGPhEA and GeMA were shown to have poor mixing across the copolymer series, shown by a non-linear distribution of specific ions (C6H5O- and C4H9+) respectively.

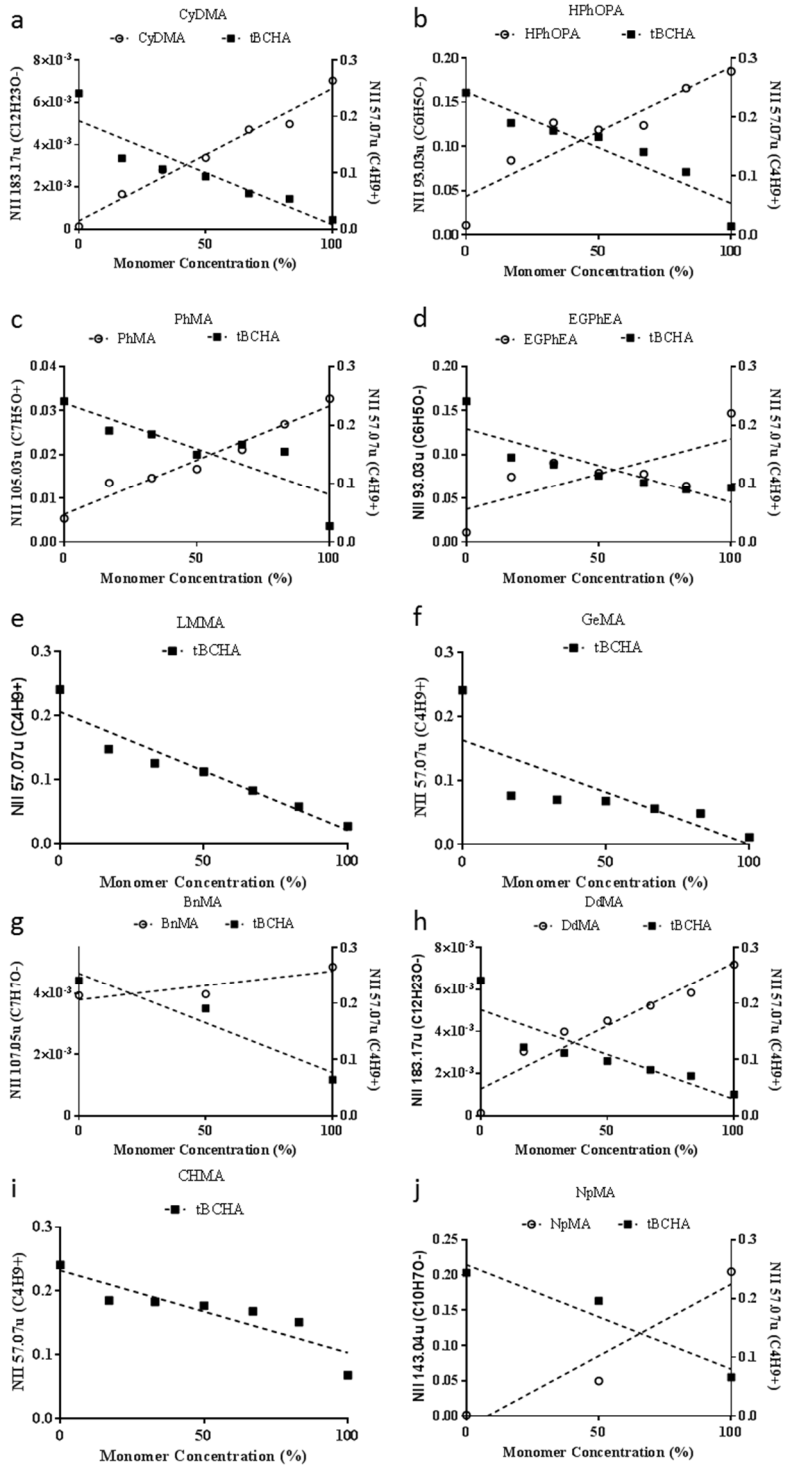

Figure S8: Series of diagrams showing mixing of copolymer series where ■ designates ion associated to tBCHA ($C_4H_9^+$) and ● designates an ion associated to a) CyDMA ($C_{12}H_{23}O^-$) b) HPhOPA ($C_6H_5O^-$) c) PhMA ($C_7H_5O^-$) d) EGPhEA ($C_6H_5O^-$) e) LMMA f) GeMA g) BnMA ($C_7H_7O^-$) h) DdMA ($C_{12}H_{23}O^-$) i) CHMA or j) NpMA ($C_{10}H_7O^-$). In the plots e, f and I, no unique secondary ion could be identified for GeMA, LMMA and CHMA

respectively likely due to the hydrocarbon structures being very similar to the co-monomer tBCHA. Copolymer series which had poor mixing (EGPhEA and GeMA) were not compared with *alpha*. tBCHA was shown not to vary across the GeMA series and the levels of both tBCHA and EGPhEA appeared to remain constant throughout the copolymer series.

We determined that leaching alcohol residuals from in-house synthesized monomers had no toxic effects on the growth of *P. aeruginosa* PAO1. Under Argon atmosphere, 20 µL of 1 % (w/v) DMPA photoinitiator in monomer (CyDMA, DdMA, GeMA, LMMA and tBCHA) was transferred into separate wells of a 96-well plate in triplicates. The plate was then irradiated with a long wave UV for 1 h under Argon and vacuum dried for 7 days. An overnight primary culture of *P. aeruginosa* grown in 10 mL LB at 37 °C and 200 rpm, was standardized to an OD_{600} of 0.01 in stock LB. 200 µl was transferred into test wells. Growth (optical density at 600 nm) was measured every 30 min over 24 h at 37 °C in Tecan Genios Fluo instrument under static conditions.

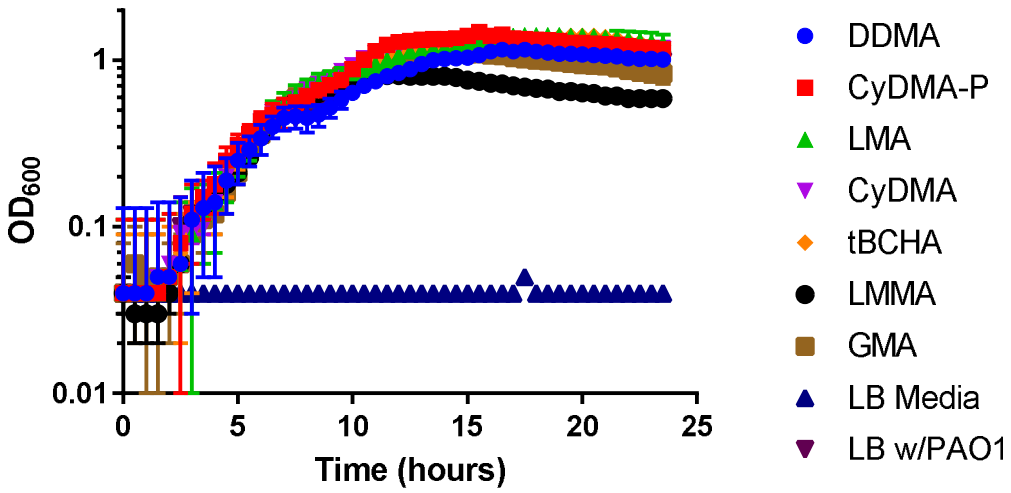

Figure S9: Optical density (OD_{600}) measurements taken over 24 hours. LB medium and LB medium innoclulated with PAO1 were used as negative and positive controls respectively. Measurements are made from n = 3 biological replicates.

Figure S9 shows that synthesised polymers (pCyDMA, pDdMA and pGeMA) all promoted PAO1 growth comparable to that of LB control with bacteria only. This suggested that the residual alcohol within the polymers was not altering bacteria growth in culture experiments. However, LMMA was excluded from any scale-up experimentation as it showed a slight decrease in the bacterial growth when compared to the control, possibly due to excess alcohol resulting from lower conversion. Secondly, purified CyDMA allowed for the same bacterial growth as both the control and the impure CyDMA, suggesting that polymers with have a high conversion and consequently low residual alcohol do not alter bacterial growth.

Further toxicity tests were performed to examine the effect of other residual alcohols and unpolymerised monomers on growth of bacteria. BMA, butanol, dodecanol and lauryl methacrylate were introduced into test plates of a 96-well plate at concentrations from 0.01 µl/ml to 1 µl/ml in fivefold increments. A total volume of 200 µl per well was reached

through addition of LB inoculated with PAO1 at OD_{600} 0.01. Growth (optical density at 600 nm) was measured every 30 min over 24 h at 37 °C in Tecan Genios Fluo instrument under static conditions.

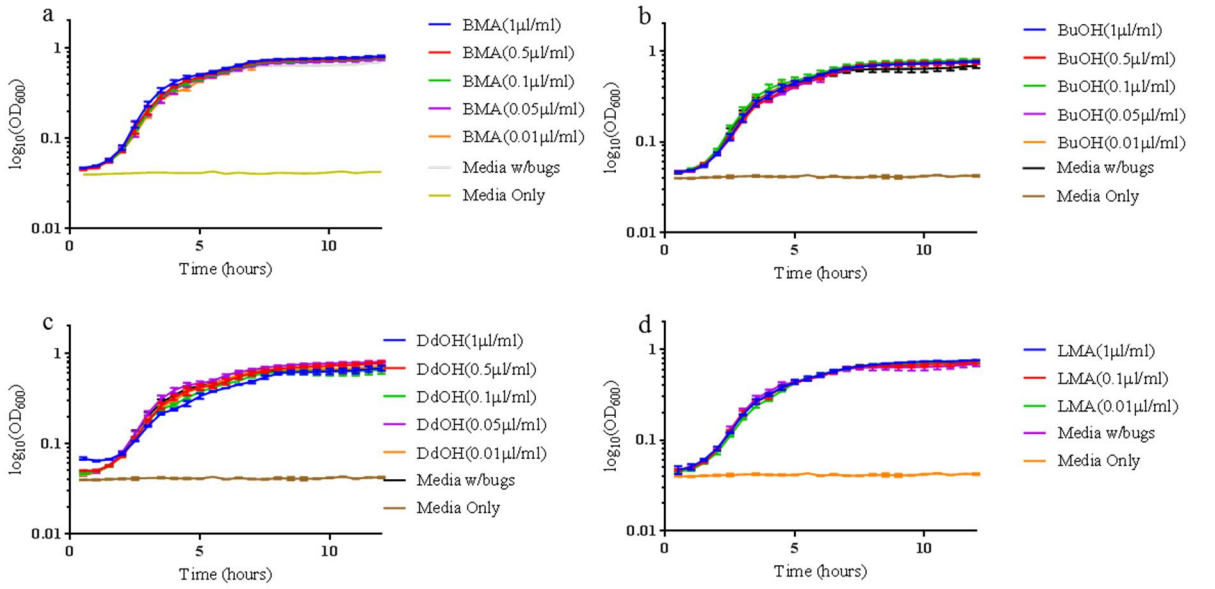

Figure S10: Toxicity assay performed using (a) BMA (b) Butanol (c) Dodecanol and (d) Lauryl methacrylate. Growth of bacteria was measured every 30 min with n = 3 biological repeats for each sample.

Concentrations selected were based upon a possible worst-case scenario assuming all of starting material stayed unreacted or unpolymerized for all the spots on a polymer microarray (2000 spots with each spot approximately 1 nL in volume) is incubated using 20 ml of RPMI media resulting in concentration of 0.1 µL/ml. It was observed that there was no effect on the bacteria with increasing concentration of starting reagents or unpolymerized lauryl methacrylate. There is a slight deviation with high concentrations of dodecanol during the log phase of bacterial growth, however this was shown to not be statistically different from the growth of bacteria in medium alone. Growth curves shown in **Figure S11** were acquired using both catalysts; titanium butoxide (TNBT) and cobalt oxime boron fluoride (COBF) with all 6

relevant pathogens. Catalyst concentrations were chosen to represent the largest expected amount of leaching of material into the inoculated media.

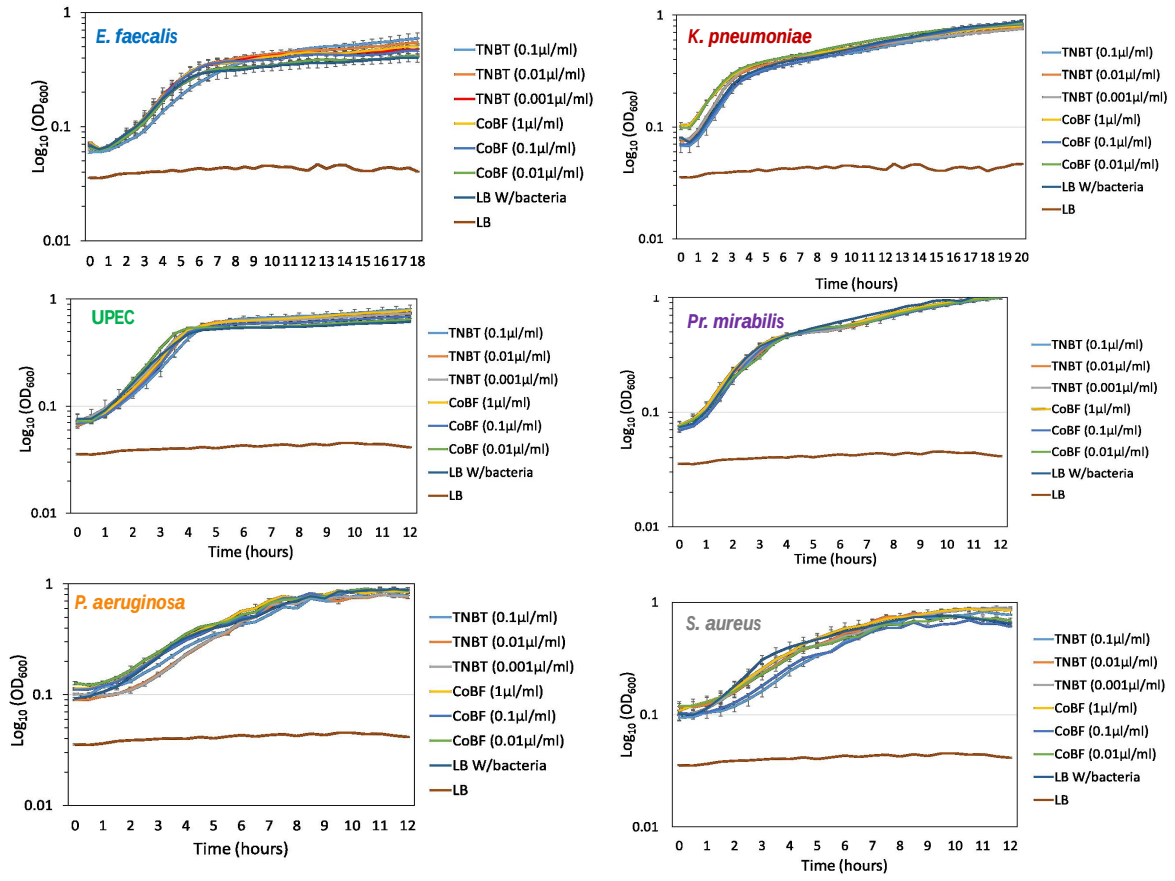

Figure S11: Growth curves showing effect of the two different used catalysts Titanium butoxide (TNBT) and cobalt oxime boron flouriode (COBF) which were used for transesterification and polymerisation processes respectively.

As shown in **Figure S11** there was no observed toxicity due to the catalysts at these range of concentrations. To determine whether monomer leeching could influence the bacterial data acquired, the three scale up monomers (CyDMA, EGDPEA and NGPDA) were tested against all 6 pathogens shown in **Figure S12**. Monomer concentrations were chosen to represent the largest expected amount of leaching of material into the inoculated media.

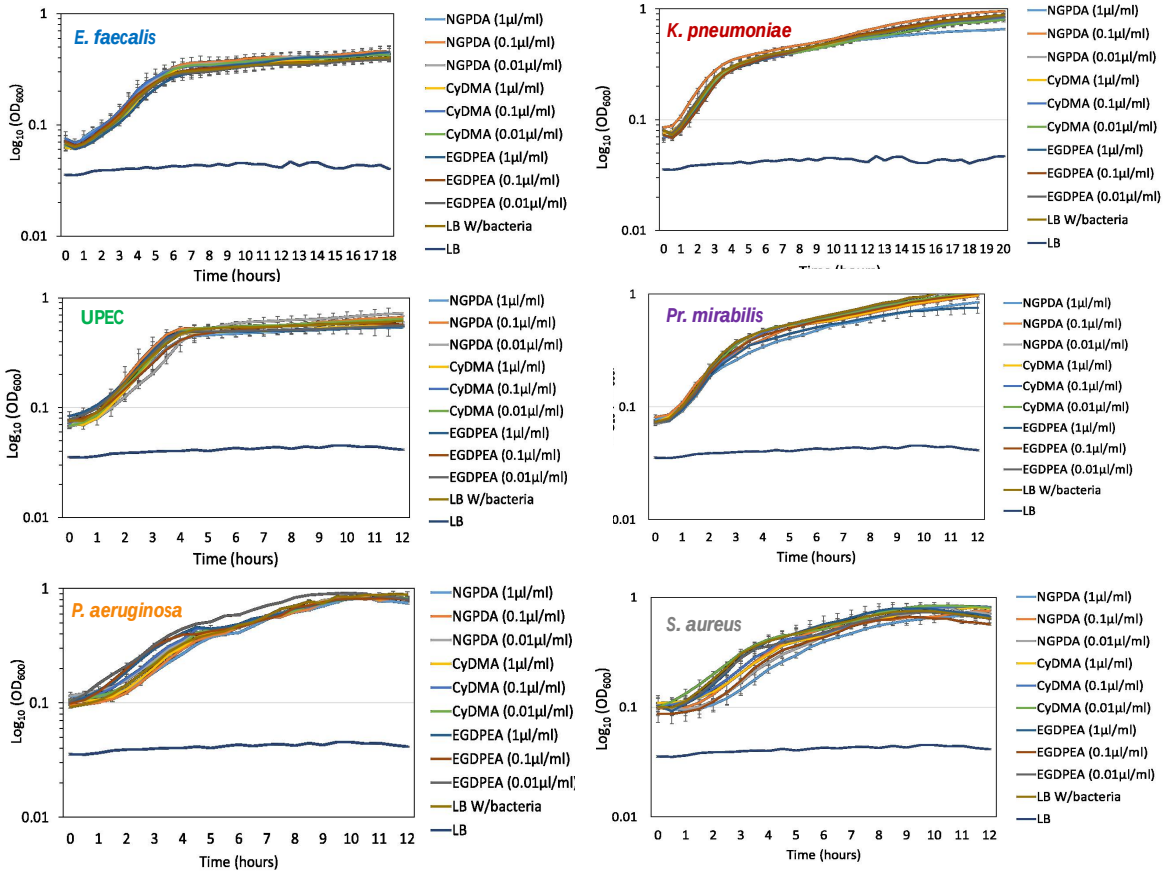

Figure S12: Growth curves showing effect of the three scale up monomers at different concentrations (0.01, 0.1 anmd 1 µl/ml) on all six pathogen species.

Figure S12 shows that there were no toxicity effects up to 1 µl/ml for any of the three monomers on all 6 pathogen species. This demonstrated that the anti-biofilm adhesion effects shown in **Figure 3** are not due to any possible toxicity effects from monomer leaching.

Investigating the effect of porcine liver esterase (PLE) on poly(Benzyl methacrylate)

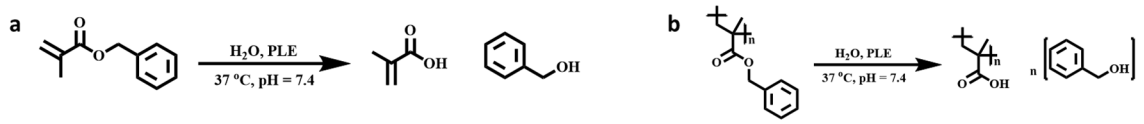

Figure S13: a) Chemical equation for degradation of Benzyl methacrylate by PLE to give Methacrylic acid and Benzyl alcohol. b) Chemical equation for degradation of p(BnMA) by PLE to give poly(methacrylic acid) and Benzyl alcohol.

We investigated the effect of quick acting PLE on a suitable anti-biofilm methacrylate polymer. The polymer of benzyl methacrylate (pBnMA) had previously been reported to exhibit broad spectrum anti-attachment resistance to pathogens including *E. Coli*, *S. aureus* and *P. aeruginosa* [4]. However, a good biological performance alone was not sufficient for this particular investigation, it was equally important for pendant group to be both soluble in water and detectable by UV, which are properties possessed by the pendant group of BnMA. Benzyl alcohol (BnOH) is both soluble in water and UV active with contribution from aromatic ring [5].

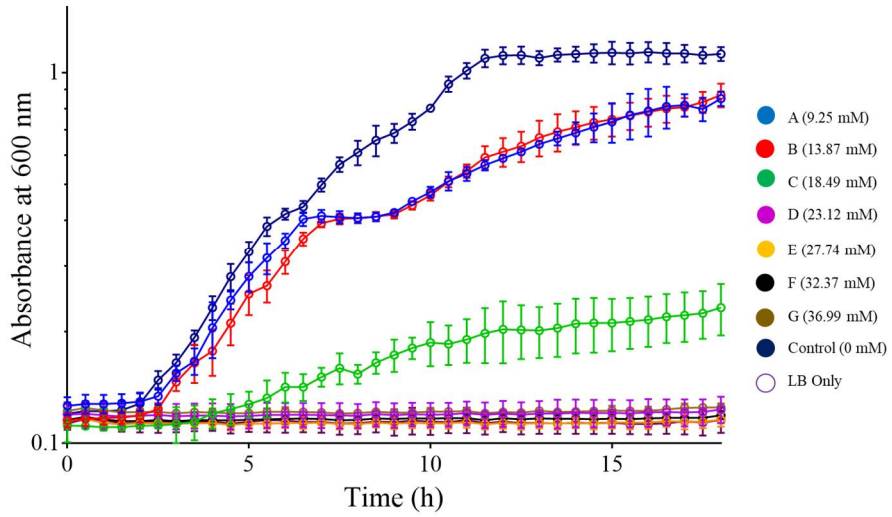

Figure S14: Growth curve of *P. aeruginosa* PAO1 incubated at 37 °C for 24 h. Error bars 1 SD, n = 3 biological replicates. ●Control, ●-A (9.25 mM), ●-B (13.87 mM), ●-C (18.49 mM), ●-D (23.13 mM), ●-E (27.74 mM), ●-F (32.37 mM), ●-G (36.99 mM) and ○- LB Only.

The toxicity to *P. aeruginosa* of potentially cleaved benzyl alcohol was tested. In **Figure S14** is the growth of PAO1 over 18 hours systematically dosed with different concentrations of BnOH. PAO1 grown in LB with no BnOH showed healthy growth over 18 h with 2.5 h in lag phase, 8 h in log and reaching stationary phase after 12 h. PAO1 dosed with 9.25 mM and 13.37 mM of BnOH showed no differences to control in the lag and log phase, a 2 hour delayed growth was however observed at time point 7.5 h, which indicated slower growth compared to control at these concentrations of BnOH. The bacteriostatic effect of BnOH was evident at 18.49 mM concentrations with very little growth observed after 18 h. There was a total inhibition of PAO1 growth at concentration beyond 18.49 mM. This suggested that the possible enzymatic cleavage of cytotoxic pendant alcohols may account for the mechanistic action of biofilm resistant materials. Albeit, this toxic effect is only achievable at high concentrations of BnOH, three orders of magnitude higher than actual experimental

conditions used (see **Figure S9**). Again, cleavage of BnOH pendant group from the pBnMA results in the formation poly(MAA-co-BnMA) in ratios dependent on activity of esterase enzyme. Copolymers with acrylic acid contents over 40 % have previously been reported to be highly bactericidal, killing bacteria within 3 h [6]. Consequently, the hypothetical enzymatic cleavage of pBnMA would be likely to give rise to toxic compounds able to reduce bacterial biofilm formation.

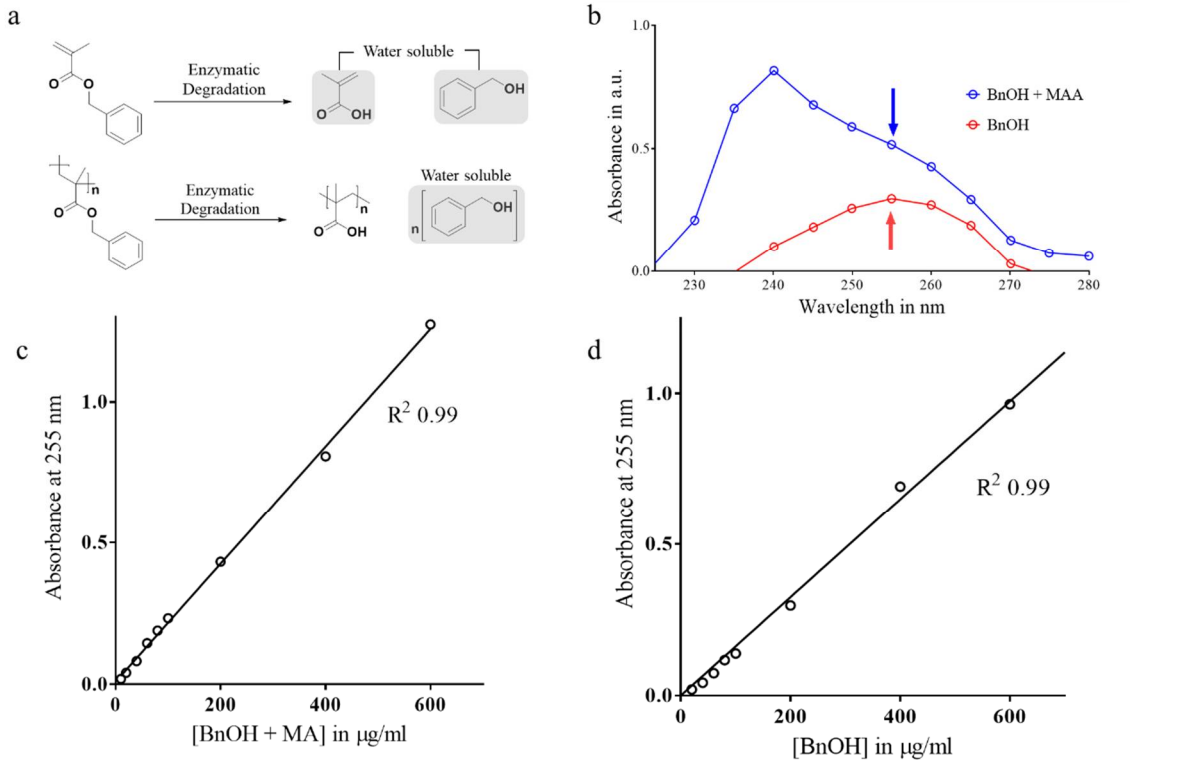

Figure S15 a) Scheme of enzymatic degradation products for pBnMA and BnMA. Water soluble products are shaded in grey. b) UV absorbance spectrum (225 – 280 nm) for BnOH (1.85 mM) in red and co-solutions of 2.32 mM MAA + 1.85 mM BnOH in blue. Arrows at 255 nm indicate wavelength used for calibration curves. c) Absorbance at 255 nm for different concentrations of BnOH + MAA. Each data point is mean ±1 s.d. N=3. d) Same convention as (c) but for BnOH.

Two different calibration curves were constructed, one to quantify the water-soluble degradation product of pBnMA that is BnOH and the second to quantify water soluble degradation products of BnMA monomer, which are BnOH and Methacrylic acid (MAA) (**Figure S15**). Coloured with red in **Figure S15b** is the absorbance spectra for BnOH with an absorbance maximum (λ_{max}) at 255 nm due to aromatic ring. The co-solutions of BnOH and MAA coloured in blue showed maximum absorbance at 240 nm. Calibration curves in **Figure S15** were constructed by measuring absorbance at 255 nm for each sample at various concentrations. Concentrations below 10 µg/mL gave inconsistent readings over experimental repeats and limit of detection (lod) for these experiments was calculated to be 40 µg/mL (400 ppm).

The λ_{max} of BnOH at 255 nm (**Figure S15b**) agreed with values reported in literature and for co-solutions of BnOH and MAA, λ_{max} was at 240 nm. The absorbance spectrum for MAA only has a reported λ_{max} at 220 nm in literature. [5] It is thought that the presence of MAA broadens the absorbance spectrum of BnOH which in turn causes a red shift for λ_{max} of MAA, from 220 nm to 240 nm.

To test the effect of PLE on polymer, BnMA was thermally polymerised to pBnMA following methods reported in experimental section for CyDMA and NMR analysis was used to confirm the absence of residual BnMA monomer.

PLE is a water soluble enzyme with a catalytic triad of serine, histidine and aspartate. Using UV absorbance at 255 nm, we studied its stability at 37 °C over a 6-day period. Results in **Figure S16a** showed that a solution of PBS alone gave readings below the zero baseline (PLE

dissolved in PBS) over a period of six days, which indicated PLE enzyme absorbed at 255 nm as expected due to aromatic amino acids. Negative readings were also recorded for pBnMA in PBS which in turn showed the insolubility of pBnMA in PBS. The monomer of BnMA also displayed constant readings below the baseline for six days. Its less negative absorbance value compared to PBS suggested trace amounts of solubilized BnMA below LOD of 400 ppm. This is in line with reported poor solubility for BnMA, estimated at 390 ppm in water at 75 °C. [7] UV absorbance for PLE enzyme is seen to be stable at baseline for first 24 hours after which an increased absorbance at 255 nm is measured. After 96 hours, the PLE enzyme had aggregated/denatured and solution turned cloudy/white. Since pH of solution remained unaltered at 7.4, we clarified that prolonged exposure to 37 °C caused conformational changes in PLE enzyme. These stability studies revealed PLE could be used in experimental procedures for up 24 hours and remain stable.

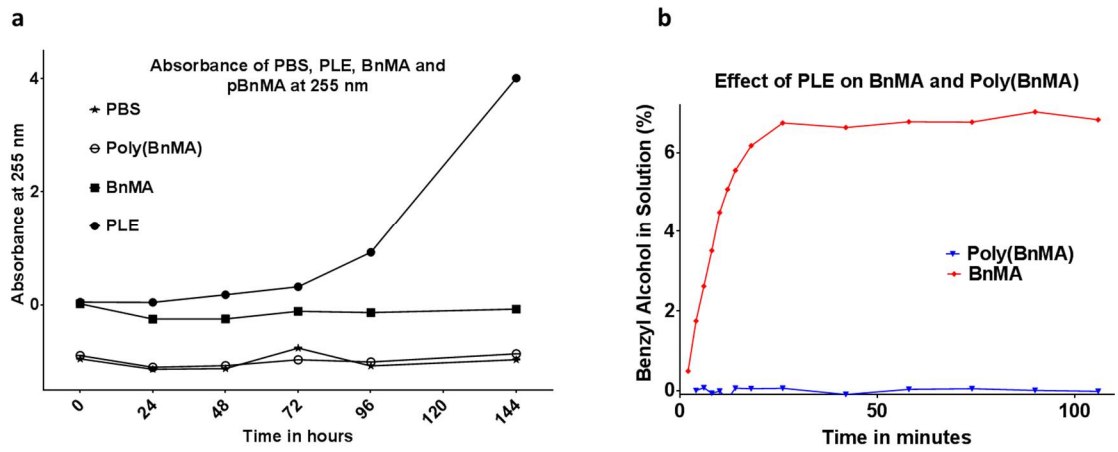

Figure S16: a) Changes in 255 nm absorbance of pBnMA, BnMA and PLE in PBS over 144 hours at 37 °C, each point is mean ± 1, n = 3. b) Degradation effect of PLE on BnMA monomer and pBnMA over 120 minutes at 37 °C, reported as percentage (wt/wt) BnOH in solution. Each point is mean ± 1, n = 3.

The data in **Figure S16b** showed that PLE has a rapid onset of action with over 6 % (wt/wt) of BnMA degraded within 25 min. PLE degraded BnMA at a rate of 44.85 µg/min for first 10 min, this reduced to 26.75 µg/min in the subsequent 4 min, followed by a rate of 10 µg/min in the succeeding 8 min. Degradation was observed to plateau after 25 min, with the clear solution turning cloudy in line with PLE aggregation caused by pH change from 7 to 4 which was attributed to the release of MA monomer at 600 µg/ml, rather than the prolonged exposure to 37 °C as seen in optimisation experiments in Figure S20a. Despite the rapid onset of PLE action, its activity against pBnMA over 2 h is not apparent. The absorbance at 255 nm is constant and close to baseline with no observable pattern of change over the duration of experiments.

It has been demonstrated that PLE is capable of cleaving over 6 % (wt/wt) of BnMA monomer in less than 30 min under the static conditions applied in this study. It is predicted that this degradation should go to 100 % (wt/wt) completion in flow conditions, where fresh PLE can be introduced into the system and denaturation avoided. Cleavage of BnMA monomer demonstrates that the test procedure developed in this study is functional. Thus, there is no evidence to suggest degradation of pBnMA by PLE within the limit of detection of this process (40 µg/ml). This indicates that either the increased steric and/or the electronic stability of the ester moiety in the polymer prevents cleavage of the ester functionality in the polymer. This data provides supporting evidence that the mechanism of action of the novel poly(acrylates) with biofilm resistant properties previously reported by the authors is not via cleavage of the ester moiety.

Copolymer surface-bacterial relationships were observed using polymer microarrays, where the correlation between the *alpha* parameter and bacterial fluorescence was observed to test the robustness of the QSAR described by *alpha*. **Figure S17** shows the weak trend associated with *S. aureus*. However, it was observed that for low *alpha* values, low bacterial adhesion to polymeric surfaces can be observed, but at higher *alpha* values, a deviation from the model was observed. This suggests despite a poor trend, similarities can be observed between the attachment of *P. aeruginosa* and *Pr. mirabilis*.

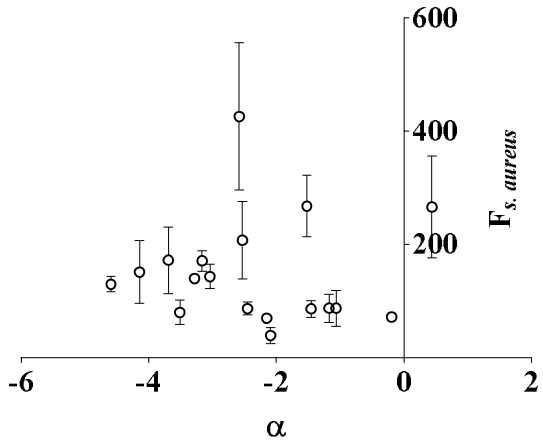

Figure S17: *S. aureus* relationship with *alpha*, $R^2 = 0$, error bars are shown with n = 3 repeats.

Figure S18 shows the quantification of the mixed biofilm species which was formed from both *P. aeruginosa* and *S. aureus*.

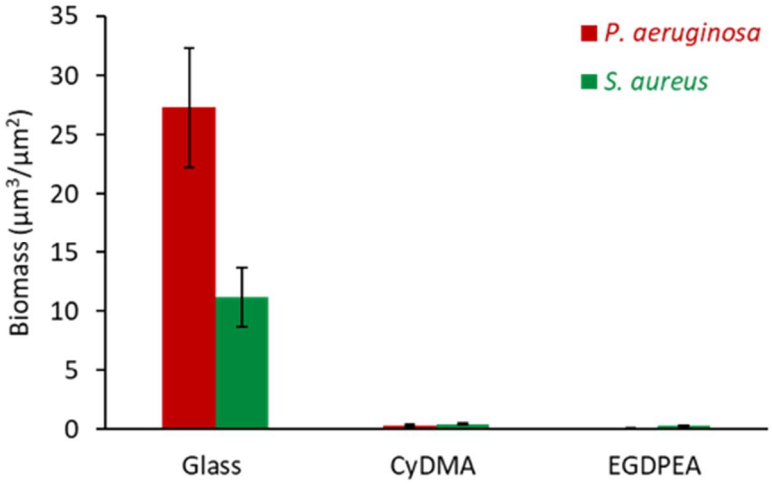

Figure S18: Resistance of CyDMA to mixed species biofilm formation in AU (Artificial Urine). Determination of the biomass of *P. aeruginosa* and *S. aureus* in mixed biofilm formed on glass, CyDMA or on EGDPEA.

This gave a biomass of 0.30 ± 0.06 and 0.13 ± 0.02 $\mu m^3/\mu m^2$ for pCyDMA and pEGDPEA respectively compared to glass (27.3 ± 5.0 $\mu m^3/\mu m^2$) for *P. aeruginosa*. A biomass of 0.46 ± 0.06 and 0.30 ± 0.07 $\mu m^3/\mu m^2$ for pCyDMA and pEGDPEA respectively compared to glass (11.2 ± 2.5 $\mu m^3/\mu m^2$) for *S. aureus*. This shows the effect of both polymers to be also be able to reduce biofilm in a more realistic multi-bacterial environment.

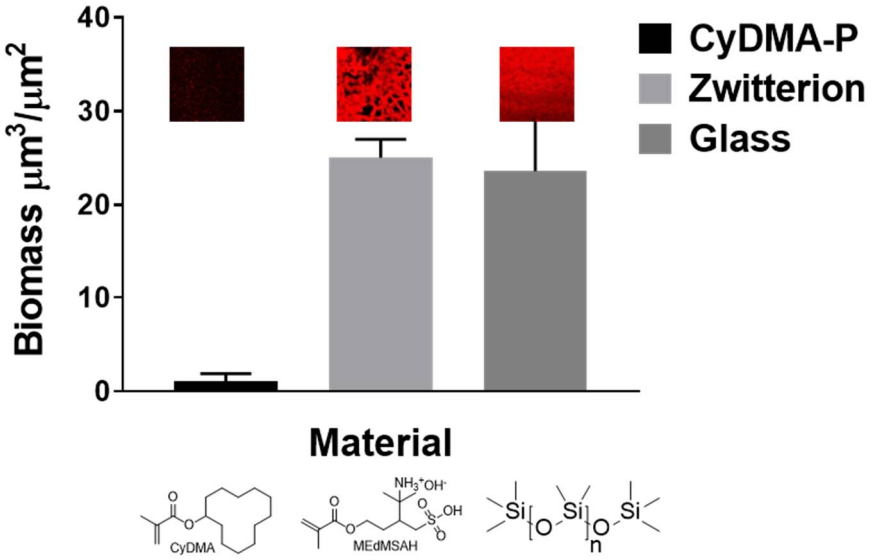

Figure S19: Quantification of *P. aeruginosa* on pCyDMA, pMEdMSAH (zwitterion) and Glass after 24 h incubation. Error bars represent mean +/- 1 SD (n = 3 biological replicates).

To coat sections of silicone-catheter with CyDMA, CyDMA was first purified using column chromatography using a solvent system of hexane: ethyl acetate in a 60:1 ratio. This led to an isolated fraction of CyDMA which was quantified using ^{1}H and ^{13}C NMR.

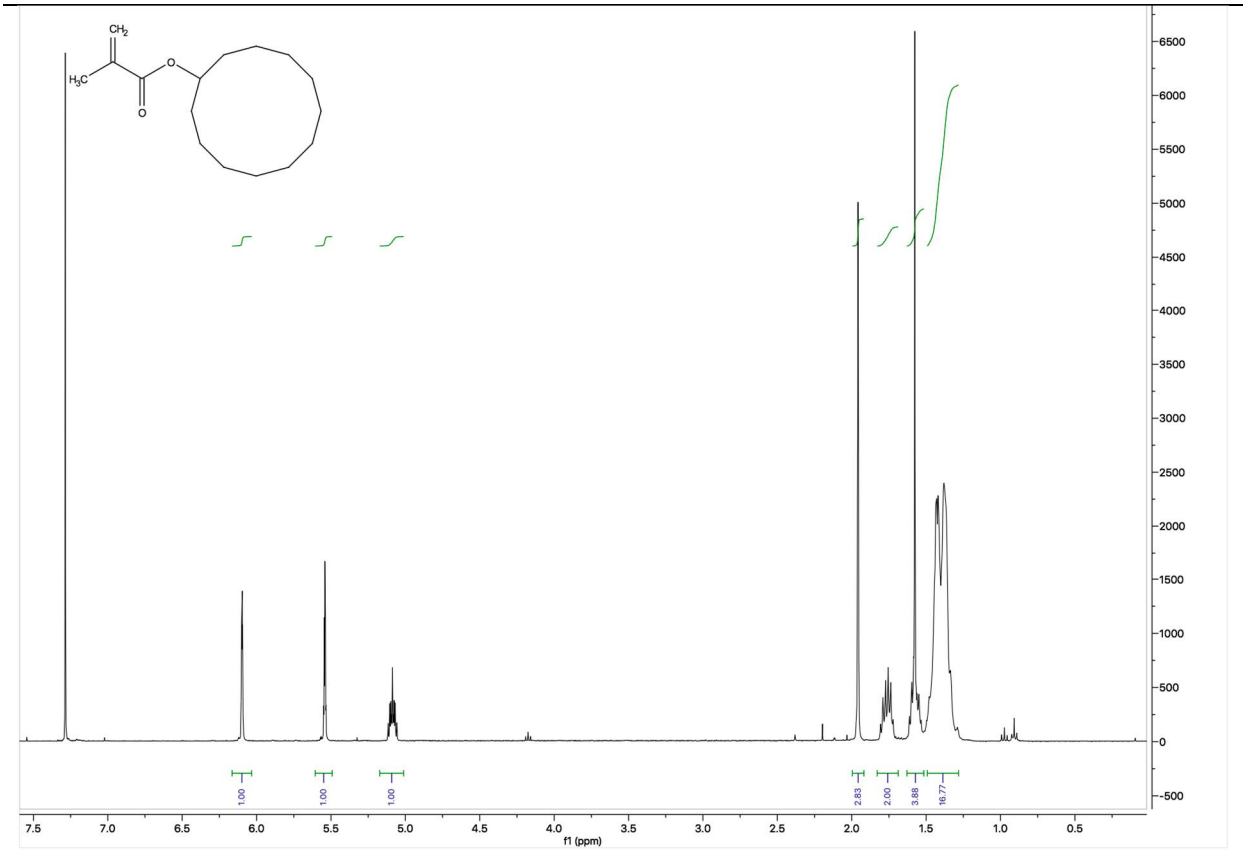

Figure S20: 1H NMR of purified CyDMA showing summation of peaks totalling a proton number of 28, corresponding to what is expected from the structure of CyDMA

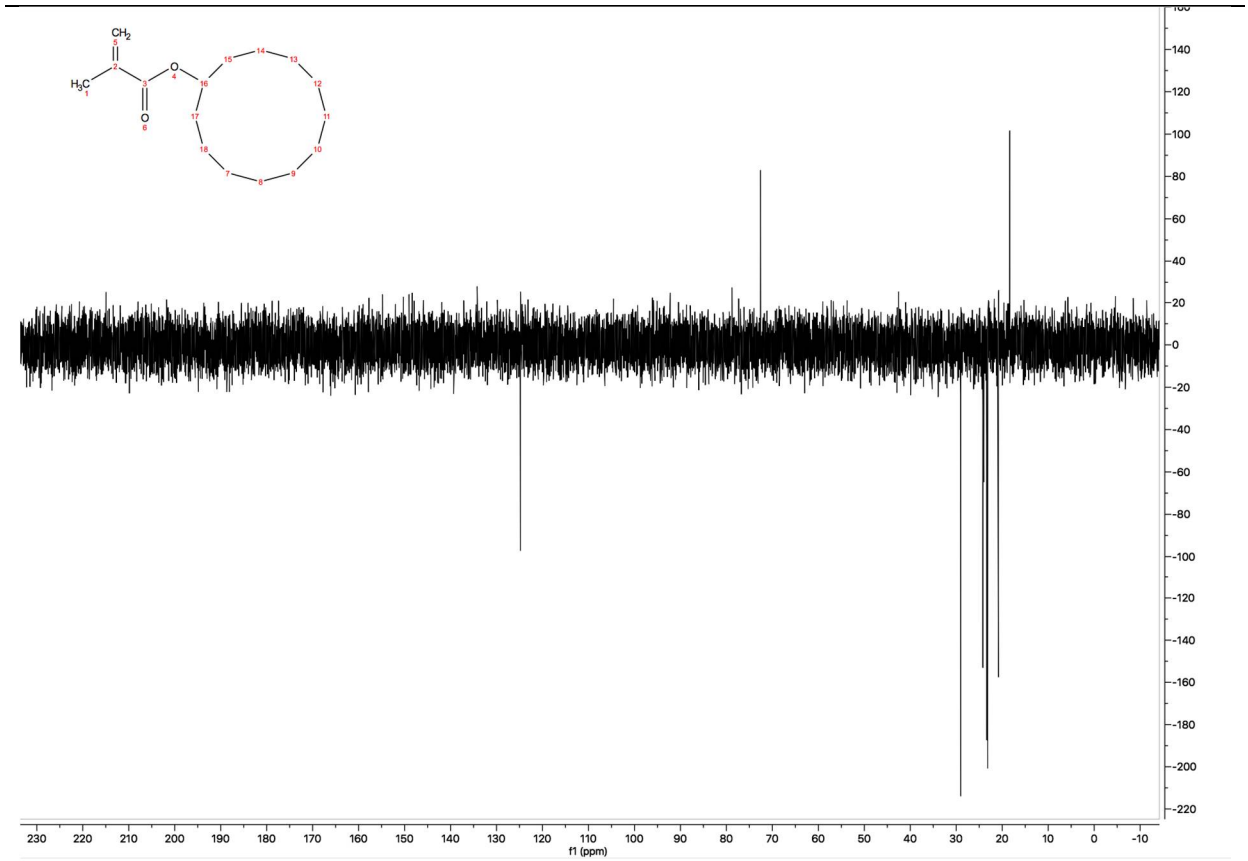

Figure S21: DEPT 135 spectrum showing assigned carbon numbers to CyDMA spectra, showing only 2 peaks for CH and CH_3 peaks as would be expected from the structure of CyDMA.

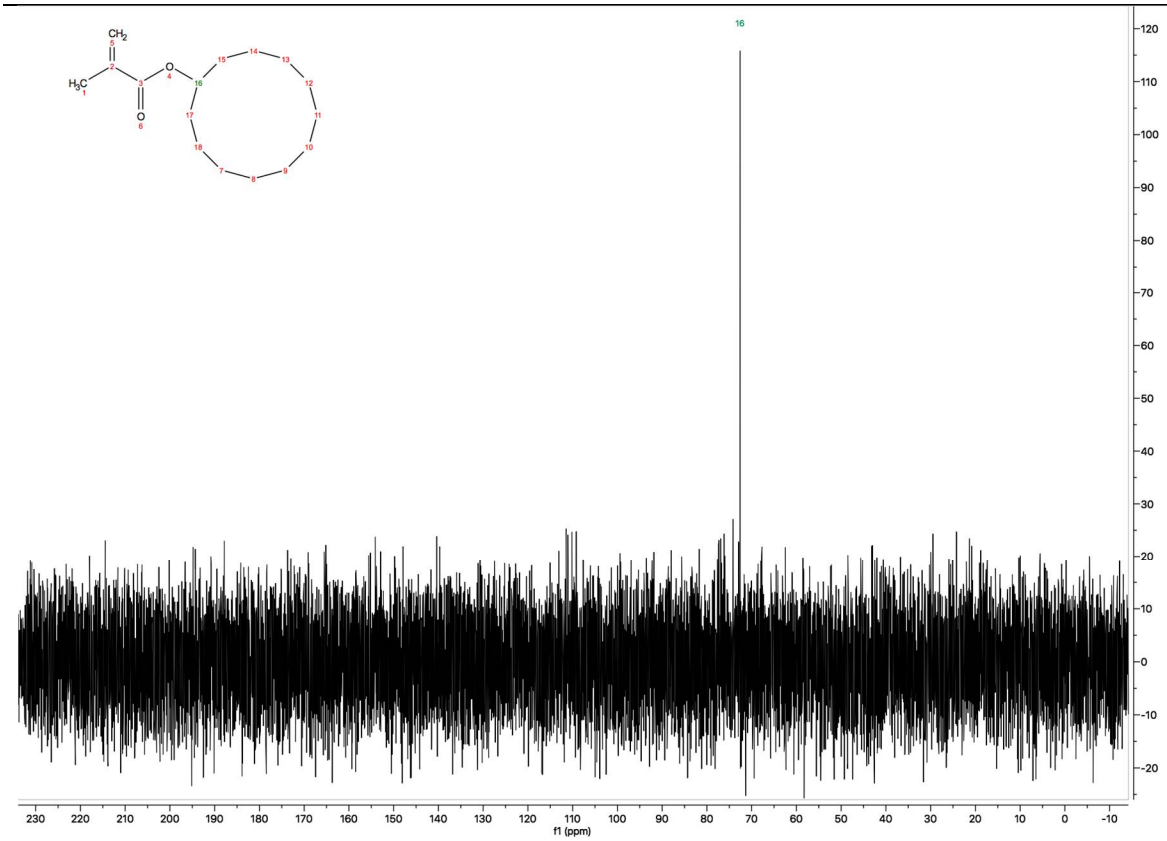

Figure S22: DEPT90 NMR spectrum showing the most deshielded postiive peak from DEPT135 spectrum is CH peak, which by viewing the structure of CyDMA is the proton that changes chemical environment during transesterification process

1. Hook, A.L., et al., *Polymer Microarrays for High Throughput Discovery of Biomaterials.* J. Visualized Exp. 2012(59): p. e3636.
2. Anderson, D.G., S. Levenberg, and R. Langer, *Nanoliter-scale synthesis of arrayed biomaterials and application to human embryonic stem cells.* Nat Biotechnol, 2004. **22**(7): p. 863-6.
3. Brooks, T. and C.W. Keevil, *A simple artificial urine for the growth of urinary pathogens.* Letters in Applied Microbiology, 1997. **24**(3): p. 203-206.
4. Hook, A.L., et al., *Discovery of novel materials with broad resistance to bacterial attachment using combinatorial polymer microarrays.* Adv Mater, 2013. **25**(18): p. 2542-7.
5. Banerjee, S., *Solubility of Organic Mixtures in Water.* Environmental Science & Technology, 1984. **18**(8): p. 587-591.
6. Gratzl, G., et al., *Antimicrobial activity of poly(acrylic acid) block copolymers.* Mater Sci Eng C Mater Biol Appl, 2014. **38**: p. 94-100.
7. Cockram, A.A., et al., *Effect of Monomer Solubility on the Evolution of Copolymer Morphology during Polymerization-Induced Self-Assembly in Aqueous Solution.* Macromolecules, 2017. **50**(3): p. 796-802.